Inorg. Chem. **2008**, *47*, 381–390

Reactivity and Catalytic Activity of a Robust Ruthenium(II)–Triphos Complex

Adrian B. Chaplin and Paul J. Dyson*

Institut des Sciences et Ingénierie Chimiques, Ecole Polytechnique Fédérale de Lausanne (EPFL), CH-1015 Lausanne, Switzerland

Received September 10, 2007

The ruthenium(II)–triphos acetato complex [RuCl(OAc)(κ^3-triphos)] (triphos = $(PPh_2CH_2)_3CMe$) has been found to be an active catalyst precursor for the hydrogenation of 1-alkenes under relatively mild conditions (5–50 bar H_2, 50 °C). In contrast to related triphenylphosphine complexes, [RuCl(OAc)(κ^3-triphos)] is much less air sensitive and high catalytic activities were achieved when catalyst samples were prepared without exclusion of air or moisture. Substitution of the acetato ligand can be effected by treatment of acid, affording $[Ru_2(\mu\text{-}Cl)_3(\kappa^3\text{-triphos})_2]Cl$ and $[RuCl(\kappa^3\text{-triphos})]_2(BF_4)_2$ with aqueous HCl and $[Et_2OH]BF_4$, respectively, or by heating with dmpm in the presence of $[NH_4]PF_6$, resulting in formation of $[RuCl(\kappa^2\text{-dmpm})(\kappa^3\text{-triphos})]PF_6$ (dmpm = $PMe_2CH_2PMe_2$). A hydride complex, [RuHCl(κ^3-triphos)], formed by acetato-mediated heterolytic cleavage of dihydrogen is proposed as the active catalytic species. An inner-sphere, monohydride mechanism is suggested for the catalytic cycle, with chloro and triphos ligands playing a spectator role. These mechanistic proposals are consistent with reactivity studies carried out on [RuCl(OAc)(κ^3-triphos)] and [RuH(OAc)(κ^3-triphos)] and supported by a computational analysis. The solid-state structures of [RuCl(OAc)(κ^3-triphos)], $[RuCl(\kappa^3\text{-triphos})]_2(BF_4)_2$, and $[RuCl(\kappa^2\text{-dmpm})(\kappa^3\text{-triphos})]PF_6$ have been established by X-ray diffraction.

Introduction

Tripodal triphosphine ligands have found widespread applications in coordination chemistry.[1] Among these ligands, the C_3-symmetric 1,1,1-tris(diphenylphosphinomethyl)ethane (triphos) and its derivatives are the most extensively investigated, forming a large variety of transition-metal complexes, many of which have found applications in catalysis.[1,2] Bianchini and co-workers, in particular, pioneered the use of this ligand in transition-metal catalysis using platinum group metals for a number of processes, including hydrogenation and hydroformylation of alkenes,[3] hydrogenation of *N*-heterocycles,[4] oxidation of catechols,[5] coupling reactions of alkynes,[6] and hydrogenation, hydrogenolysis, and hydrodesulfurization of thiophenes.[7] Functionalization of the triphos ligand by derivation of the bridgehead atom with

* To whom correspondence should be addressed. E-mail: paul.dyson@epfl.ch.

(1) (a) Hierso, J.-C.; Amardeil, R.; Bentabet, E.; Boussier, R.; Gautheron, B.; Meunier, P.; Kalck, P. *Coord. Chem. Rev.* **2004**, *236*, 143. (b) Mayer, H. A.; Kaska, W. C. *Chem. Rev.* **1994**, *94*, 1239. (c) Cotton, F. A.; Hong, B. *Prog. Inorg. Chem.* **1992**, *40*, 179.

(2) (a) Chaplin, A. B.; Dyson, P. J. *Eur. J. Inorg. Chem.* **2007**, 4973. (b) Magro, A. A. N.; Eastham, G. R.; Cole-Hamilton, D. J. *Chem. Commun.* **2007**, 3154. (c) Rosales, M.; Vallejo, R.; Soto, J. J.; Chacón, G.; González, A.; González, B. *Catal. Lett.* **2006**, *106*, 101. (d) Rosales, M.; González, A.; González, B.; Moratinos, C.; Pérez, H.; Urdaneta, J.; Sánchez-Delgado, R. A. *J. Organomet. Chem.* **2005**, *690*, 3095. (e) Chen, J.-X.; Daeuble, J. F.; Brestensky, D. M.; Stryker, J. M. *Tetrahedron* **2000**, *56*, 2153. (f) Sung, K.-M.; Huh, S.; Jun, M.-J. *Polyhedron* **1999**, *18*, 469. (g) Teunissen, H. T.; Elsevier, C. J. *Chem. Commun.* **1998**, 1367. (h) Sernau, V.; Huttner, G.; Friz, M.; Zsolnai, L.; Walter, O. *J. Organomet. Chem.* **1993**, *453*, C23. (i) Bianchini, C.; Meli, A.; Peruzzini, M.; Vizza, F.; Zanobni, F. *Coord. Chem. Rev.* **1992**, *120*, 193. (j) Ott, J.; Tombo, G. M. R.; Schmid, B.; Venanzi, L. M.; Wang, G.; Ward, T. R. *Tetrahedron Lett.* **1989**, *30*, 6151. (k) Suarez, T.; Fontal, B. *J. Mol. Catal.* **1985**, *32*, 191.

(3) (a) Bianchini, C.; Meli, A.; Peruzzini, M.; Vizza, F.; Frediani, P.; Frediani, P.; Ramirez, J. A. *Organometallics* **1990**, *9*, 226. (b) Bianchini, C.; Meli, A.; Peruzzini, M.; Vizza, F.; Fujiwara, Y.; Jintoku, T.; Taniguchi, H. *J. Chem. Soc., Chem. Commun.* **1988**, 299. (c) Bianchini, C.; Meli, A.; Laschi, F.; Ramirez, J. A.; Zanello, P. *Inorg. Chem.* **1988**, *27*, 4429.

(4) (a) Barbaro, P.; Bianchini, C.; Meli, A.; Moreno, M.; Vizza, F. *Organometallics* **2002**, *21*, 1430. (b) Bianchini, C.; Barbaro, P.; Macchi, M.; Meli, A.; Vizza, F. *Helv. Chim. Acta* **2001**, *84*, 2895.

(5) (a) Barbaro, P.; Bianchini, C.; Frediani, P.; Meli, A.; Vizza, F. *Inorg. Chem.* **1992**, *31*, 1523. (b) Barbaro, P.; Bianchini, C.; Mealli, C.; Meli, A. *J. Am. Chem. Soc.* **1991**, *113*, 3181. (c) Bianchini, C.; Frediani, P.; Laschi, F.; Meli, A.; Vizza, F.; Zanello, P. *Inorg. Chem.* **1990**, *29*, 3402.

(6) Bianchini, C.; Meli, A.; Peruzzini, M.; Vacca, A.; Vizza, F. *Organometallics* **1991**, *10*, 645.

(7) (a) Bianchini, C.; Meli, A.; Vizza, F. *J. Organomet. Chem.* **2004**, *689*, 4277. (b) Bianchini, C.; Meli, A. *J. Chem. Soc., Dalton Trans.* **1996**, 801. (c) Bianchini, C.; Meli, A. *Acc. Chem. Res.* **1998**, *31*, 109.

10.1021/ic701773a CCC: $40.75
Published on Web 11/29/2007

Scheme 1

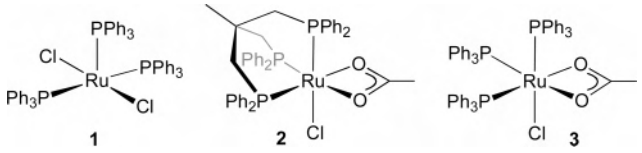

Scheme 2. Preparation of **2** and **4**

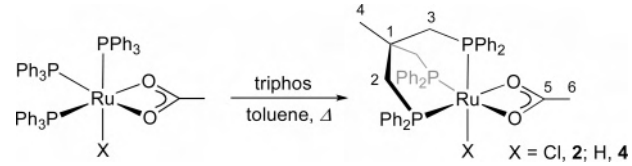

appropriate moieties has allowed formation of metallodendrimers[8] or immobilization of metal complexes into/onto silica,[9] polymers,[10] or biphases,[11] facilitating catalyst reuse or modifying reactivity. Such immobilization is complemented by the tridentate nature of the ligand, stabilizing the metal center during catalysis and reducing leaching.

Despite extensive use of ruthenium(II)−phosphine complexes in hydrogenation,[12] there are few examples of well-defined ruthenium(II)−triphos complexes that catalyze this process. This paucity is somewhat surprising owing to the successful application of $[RuCl_2(PPh_3)_3]$ (**1**, Scheme 1) and related complexes containing trisphosphine ligands in hydrogenation.[12,13] The air sensitivity of **1**, as a result of facile triphenylphosphine dissociation in solution, significantly limits its application, and the increased stability provided by the tripodal nature of the triphos ligand makes it an attractive ligand for enhancing the stability of the ruthenium(II)−phosphine complexes. Well-defined ruthenium(II)−triphos complexes employed for hydrogenation include $[RuH(\kappa^2\text{-}BH_4)(\kappa^3\text{-triphos})]$,[14] $[Ru(NCMe)_3(\kappa^3\text{-triphos})]^+$,[4a,14] and $[RuHCl(CO)(\kappa^3\text{-triphos})]$.[2f] Complexes containing the functionalized triphos ligand sulfos, $(PPh_2CH_2)_3CCH_2(C_6H_4)SO_3^-$, have also been employed together with ruthenium(II) in hydrogenation.[9c,d,11a]

Building upon the highly successful application of ruthenium(II)−diphosphine acetato complexes as hydrogenation catalysts, developed by Noyori and co-workers,[15] and as part of our investigations of ruthenium(II)−phosphine complexes,[16] we report here on the reactivity and hydrogenation activity of the ruthenium(II)−triphos acetato complex (**2**, Scheme 1). Determination of the catalytic activity of **2** is supplemented by relevant mechanistic studies, a computational analysis, and comparisons to the activity of **1** and the related tris-triphenylphosphine complex $[RuCl(OAc)(PPh_3)_3]$, **3**.[17]

Results and Discussion

1. Synthesis and Characterization. Substitution of PPh_3 in **3** by triphos in toluene under reflux affords **2** in high yield (93%) as an analytically pure, air-stable solid (Scheme 2). The $^{31}P\{^1H\}$ NMR spectrum of **2** at room temperature contains two broad resonances at 40.5 and 36.7 ppm (CD_2Cl_2, 2:1 ratio), which upon progressive cooling to −10 °C sharpen into well-defined doublet and triplet resonances (40.4 and 37.0 ppm), respectively, with a $^2J_{PP}$ coupling constant of 40 Hz (Figure 1). This broadening suggests a certain degree of stereochemical nonrigidity, although coalescence was not reached within the boiling point limit of the solvent.[18] Similar behavior has been observed for a series of κ^3-triphos complexes $[Ru(L\text{-}L')(NCMe)(\kappa^3\text{-triphos})]OTf$ (L-L′ = κ^2-*S*-diorganyldithiocarbamate/κ^2-*N*,*S*-thioamide) prepared by Landgrafe and co-workers, although derivates formed by

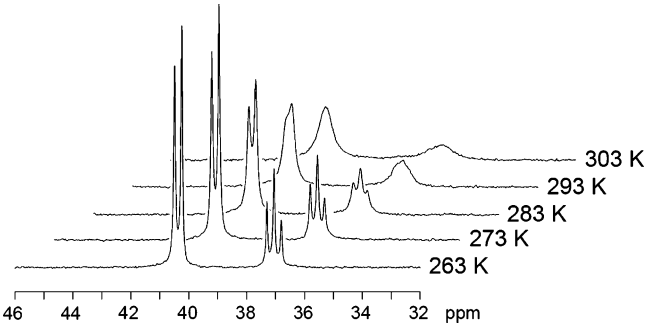

Figure 1. Variable-temperature $^{31}P\{^1H\}$ NMR (CD_2Cl_2) spectra of **2**.

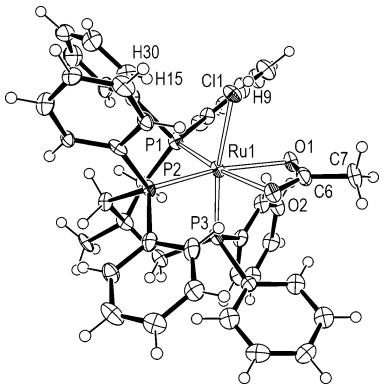

Figure 2. ORTEP representation of **2**, thermal ellipsoids drawn at 50% probability. Key bond lengths (Å) and angles (deg): Ru1−Cl1, 2.448(2); Ru1−P1, 2.277(3); Ru1−P2, 2.282(2); Ru1−P3, 2.275(2); Ru1−O1, 2.249(5); Ru1−O2, 2.198(6); Ru1−C6, 2.580(9); Ru1−C6−C7, 173.0(6); Cl1−Ru1−P1, 95.29(8); Cl1−Ru1−P2, 99.67(8); Cl1−Ru1−P3, 171.05(7); Cl1−Ru1−C6, 78.4(2); P1−Ru1−P2, 86.28(8); P1−Ru1−P3, 89.11(9); P2−Ru1−P3, 88.37(8); P1−Ru1−C6, 138.6(2); P2−Ru1−C6, 135.1(2); P3−Ru1−C6, 93.1(2); O1−Ru1−O2, 59.7(2).

(8) Findeis, R. A.; Gade, L. H. *Eur. J. Inorg. Chem.* **2003**, 99.
(9) Metal-impregnated silica: (a) Barbaro, P.; Bianchini, C.; Santo, V. D.; Meli, A.; Moneti, S.; Psaro, R.; Scaffidi, A.; Sordelli, L.; Vizza, F. *J. Am. Chem. Soc.* **2006**, *128*, 7065. (b) Bianchini, C.; Santo, V. D.; Meli, A.; Moneti, S.; Moreno, M.; Oberhauser, W.; Psaro, R.; Sordelli. L.; Vizza, F. *Angew. Chem., Int. Ed.* **2003**, *42*, 2536. Silica alone: (c) Bianchini, C.; Santo, V. D.; Meli, A.; Moneti, S.; Moreno, M.; Oberhauser, W.; Psaro, R.; Sordelli, L.; Vizza, F. *J. Catal.* **2003**, *213*, 47. (d) Bianchini, C.; Santo, V. D.; Meli, A.; Oberhauser, W.; Psaro, R.; Vizza, F. *Organometallics* **2000**, *19*, 2433. (e) Bianchini, C.; Burnaby, D. G.; Evans, J.; Frediani, P.; Meli, A.; Oberhauser, W.; Psaro, R.; Sordelli, L.; Vizza, F. *J. Am. Chem. Soc.* **1999**, *121*, 5961.
(10) Bianchini, C.; Frediani, M.; Vizza, F. *Chem. Commun.* **2001**, 479.
(11) (a) Rojas, I.; Linares, F. L.; Valencia, N.; Bianchini, C. *J. Mol. Cat. A* **1999**, *144*, 1. (b) Bianchini, C.; Frediani, P.; Sernau, V. *Organometallics* **1995**, *14*, 5458.
(12) (a) Morris, R. H. *Handbook of Homogenous Hydrogenation*; de Vries, J. G., Elsevier, C. J., Eds.; Wiley-VCH: Weinheim, 2007; Vol. 1, p 45. (b) Kitamura, M.; Noyori, R. *Ruthenium in Organic Synthesis*; Murahashi, S.-I., Ed.; Wiley-VCH: Weinheim, 2004; p 3.
(13) Evans, D.; Osborn, J. A.; Jardine, F. H.; Wilkinson, G. *Nature* **1965**, *208*, 1203.
(14) Bianchini, C.; Meli, A.; Moneti, S.; Vizza, F. *Organometallics* **1998**, *17*, 2636.
(15) Noyori, R. *Angew. Chem., Ind. Ed.* **2002**, *41*, 2008.

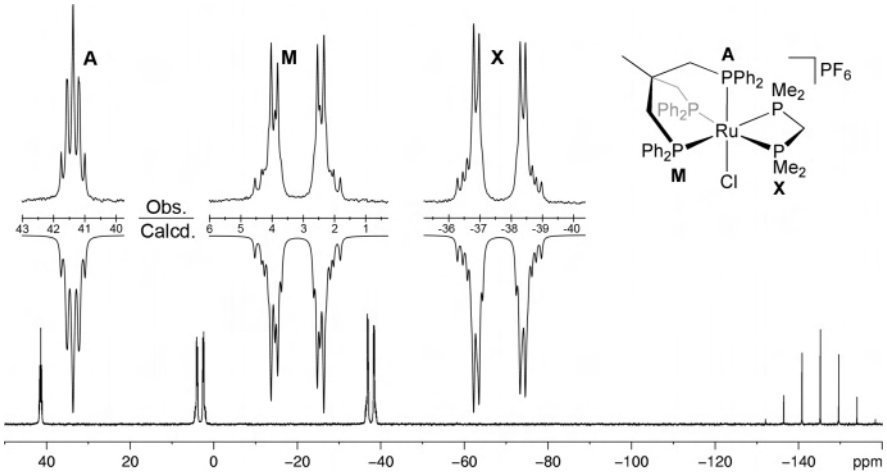

Figure 3. $^{31}P\{^1H\}$ NMR (CD_2Cl_2, 293 K) spectrum of **7** together with assignments and simulated regions.

Scheme 3

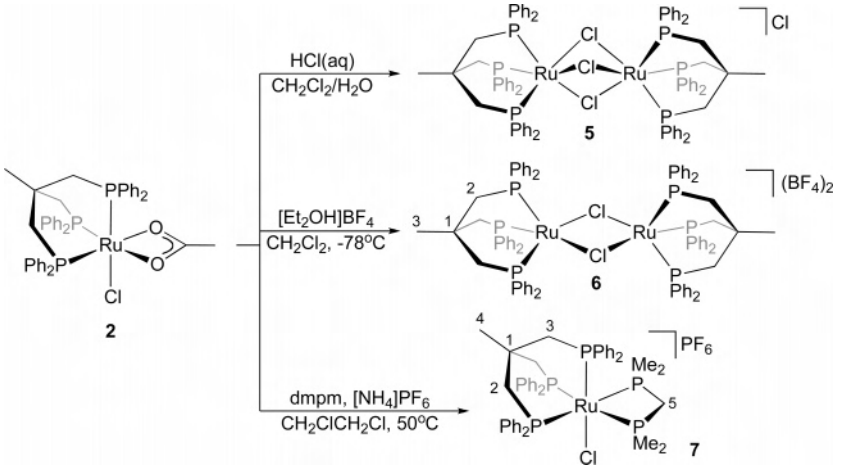

substitution of the acetonitrile ligand were found to be stereochemically rigid at ambient temperature.[19] The related hydride complex, [RuH(OAc)(κ^3-triphos)], **4**, prepared in an analogous fashion to **2** (used for mechanistic investigations described below), in contrast, exhibits sharp and well-defined resonances at room temperature in the $^{31}P\{^1H\}$ NMR spectrum. The doublet and triplet resonances are located at 61.0 and 6.2 ppm, respectively (2:1 ratio, CD_2Cl_2), and the $^2J_{PP}$ coupling constant of **4** is reduced in comparison to **2** (40 vs 20 Hz). A characteristic doublet of triplets is observed at −2.78 ppm in the ^1H NMR spectrum of **4**, with $^2J_{PH}$ coupling constants of 122 and 20 Hz.

The solid-state structure of **2** has been determined by X-ray diffraction and is depicted in Figure 2. The ruthenium center has a distorted octahedral geometry, the triphos ligand adopting the expected *fac*-geometry. The distortion from ideal octahedral geometry predominantly results from the small chelate angle of the acetato ligand [59.7(2)°] and the significant bending of the chloro ligand away from the axial axis [P3−Ru1−Cl1 = 171.05(7)°]. The bending of the chloro ligand appears to be steric in origin; three protons from the neighboring phenyl groups lie within the corresponding combined van der Waals radii (2.95 Å; H9, H15, and H39). These features are also observed in the related complex *fac*-[RuCl(OAc)(κ^3-$(PCy_2CH_2)_2PPh$)] [O−Ru−O, 58.9(1)°; P_{ax}−Ru−Cl, 170.6(1)°].[20]

2. Substitution Reactions of 2. The ability of the acetato ligand in **2** to undergo substitution on treatment of acid was demonstrated by reaction with aqueous HCl under biphasic conditions, resulting in formation of the trichloro-bridged ruthenium dimer **5**, Scheme 3. Alternatively, reaction of **2** at low temperature with $[Et_2OH]BF_4$, containing the weakly coordinating tetrafluoroborate anion, affords a 16 VE dichloro-bridged ruthenium dimer [RuCl(κ^3-triphos)]$_2(BF_4)_2$, **6**. The $^{31}P\{^1H\}$ NMR spectrum of **6** exhibits a single resonance at 55.8 ppm (CD_2Cl_2), which is also detected in low intensity initially on reaction of **2** with HCl. The structure of **6** was confirmed by ESI-MS, the presence of a molecular ion peak

(16) (a) Chaplin, A. B.; Dyson, P. J. *Organometallics* **2007**, *26*, 4357. (b) Chaplin, A. B.; Dyson, P. J. *Organometallics* **2007**, *26*, 2447. (c) Chaplin, A. B.; Fellay, C.; Laurenczy, G.; Dyson, P. J. *Organometallics* **2007**, *26*, 586. (d) Chaplin, A. B.; Scopelliti, R.; Dyson, P. J. *Eur. J. Inorg. Chem.* **2005**, 4762. (e) Geldbach, T. J.; Chaplin, A. B.; Hänni, K. D.; Scopelliti, R.; Dyson, P. J. *Organometallics* **2005**, *24*, 4974. (f) Daguenet, C.; Scopelliti, R.; Dyson, P. J. *Organometallics* **2004**, *23*, 4849.

(17) Mainz, V. V.; Andersen, R. A. *Organometallics* **1984**, *3*, 675.

(18) Estimated coalescence temperature in CD_2Cl_2 is 80 °C (from high-pressure experiments).

(19) Landgrafe, C.; Sheldrick, W. S.; Südfeld, M. *Eur. J. Inorg. Chem.* **1998**, 407.

(20) Jian, G.; Rheingold, A. L.; Haggerty, B. S.; Meek, D. W. *Inorg. Chem.* **1992**, *31*, 900.

Table 1. ^{31}P NMR Chemical Shifts and Coupling Constants for **7** Obtained by Simulation Analysis (excluding Anion Resonance)

	δ/ppm	J/Hz
A	41.4	$J_{AM} = 35$, $J_{AX} = 28$
M	3.2	$J_{MM} = 42$, $J_{MX} = 263$ (trans), $J_{MX} = 23$ (cis)
X	−37.6	$J_{XX} = -62$

at $m/z + 761$ corresponding to the dication, and single-crystal X-ray diffraction (see below). Substitution of the acetato ligand in **2** can also be effected using the basic diphosphine dmpm in the presence of $[NH_4]PF_6$, affording $[RuCl(\kappa^2\text{-dmpm})(\kappa^3\text{-triphos})]PF_6$ (**7**, dmpm = $PMe_2CH_2PMe_2$). The reaction proceeds via the presence of an intermediate species, tentatively assigned as $[Ru(\kappa^1\text{-OAc})(\kappa^2\text{-dmpm})(\kappa^3\text{-triphos})]^+$ on the basis of $^{31}P\{^1H\}$ NMR data. The coordination geometry of the phosphine ligands in **7** is confirmed by the presence of a distinct and non-first-order AMM′XX′ coupling system in the $^{31}P\{^1H\}$ NMR spectrum (Figure 3). The spectral parameters were extracted by simulation analysis and are listed in Table 1. Of note, the value of the larger J_{MX} coupling constant (263 Hz) is typical for *trans*-coordinated phosphines.[21] The coordination of the chloro ligand is confirmed by ESI-MS (**7** exhibits a strong molecular ion peak at $m/z + 897$), ^{1}H NMR spectroscopy, and single-crystal X-ray diffraction.

The solid-state structures of **6** and **7** are depicted in Figure 4. The structure of **6** contains two ruthenium centers, with distorted square pyramidal geometries, bridged by two chloro ligands. The Ru···Ru separation of 3.8732(7) Å in **6** is significantly larger than that in $[Ru_2(\mu\text{-Cl})_3(\kappa^3\text{-triphos})_2]BPh_4$ (**8**) [3.455(1) Å] owing to enlarged Ru−Cl−Ru angles [**6**, 102.49(4)°; **8**, 88.00(9)°, 87.64(11)°].[22] Both the Ru−Cl [**6**, avg. 2.49 Å; **8** avg. 2.48 Å] and the Ru−P [**6**, 2.26 Å; **8**, avg. 2.30 Å] bonds in **6** are similar to those in **8**. A similar distorted octahedral geometry to that of **2** is found for the structure of **7**; however, the Ru−Cl [**2**, 2.448(2) Å; **7**, 2.5012(11), 2.4884(11) Å] and Ru−P(triphos) [**2**, avg. 2.28 Å; **7** avg. 2.37 Å] bonds are significantly elongated in comparison. The larger bite angle [69.00(4)°, 69.99(4)°] and increased steric bulk around the donor atoms of dmpm, in comparison to that of the acetato ligand [59.7(2)°], could be partially responsible for the elongation, although electronic differences between these two ligand also may play a role.

3. Hydrogenation of Alkenes. The catalytic evaluation of **1**−**4** was performed in THF at 50 °C with a substrate to catalyst ratio of 10 000:1 using 5 or 50 bar H_2. As both **1** and **3** are air sensitive, samples were prepared under an inert atmosphere in a glove box. The results from these investigations are listed in Table 2. Although **2** was less active than the triphenylphosphine complexes (TOFs of 6400 and 8000 h^{-1} for **1** and **3**, respectively), a TOF of 3000 h^{-1} could be achieved for hydrogenation of styrene under 5 bar of H_2. Under these conditions, the hydride analogue **4** was found to be inactive and addition of mercury to catalyst solutions of **2**, as a selective poison for heterogeneous catalysts, did not inhibit the catalytic activity of **2** significantly.[23] Under higher pressure (50 bar H_2) complete hydrogenation of styrene could be achieved with **1**−**3** in 1 h (TOFs ≥ 10 000 h^{-1}). Interestingly, only **2** was detected by ^{31}P NMR spectroscopy following catalysis under these conditions, suggesting that formation of the active catalyst is reversible. If the samples were prepared in air, large reductions in activity were observed for **1** and **3** (TOFs of 200 and 900 h^{-1}, respectively), while the activity for **2** remained high (TOF of 7400 h^{-1}).

Complexes **1** and **3** both catalyzed the hydrogenation of 1-hexene under 5 bar of H_2, achieving higher conversions than those observed for styrene under the same conditions. In contrast, **2** is significantly less active, requiring 50 bar of H_2 to achieve significant conversion (TOF of 6800 h^{-1}). Both **1** and **2** showed low activity (TOFs < 300 h^{-1}) for hydrogenation of cyclohexene under 50 bar of H_2, although **3** proved to be an effective catalyst, achieving a TOF of 6200 h^{-1}.

The observed activity of **1** is in line with previous reports, which indicate that it is an extremely active catalyst precursor for terminal alkenes but poorly active for internal alkenes.[12] Conversion of **1** into the active hydride species, $[RuHCl(PPh_3)_3]$, probably involves THF-mediated intermolecular heterolytic cleavage under the conditions employed. The enhanced catalytic activity of **3**, in comparison to **1**, could be due to more facile intramolecular heterolytic cleavage, of dihydrogen assisted by the acetato ligand (in a similar manner to that described below), although the high activity for cyclohexene hydrogenation may also imply that the acetato ligand plays a more intimate role during catalysis. The mechanism of **2** for alkene hydrogenation is discussed below.

4. Mechanistic Investigations. To further establish aspects of the catalytic chemistry of **2**, reactions with dihydrogen were carried out in the absence of alkene substrates. Although no products were formed from **2** under 50 bar of H_2 at 50 °C, addition of a large excess of NEt_3 (20 equiv) resulted in an equilibrium reaction involving formation of **4**, as indicated by ^{1}H and $^{31}P\{^1H\}$ NMR spectroscopy (Scheme 4). Under 50 bar of H_2 the equilibrium ratio of **2**:**4** was 12:1, which was reduced to 10:1 on further pressurization to 80 bar of H_2. Following cooling the sample to room temperature, depressurization, and degassing, **4** reverted back to **2**. The reverse reaction, formation of **2** from **4**, could also be effected at ambient temperature in the absence of dihydrogen by reaction of **4** with NEt_3·HCl (3 equiv), affording **2** rapidly and quantitatively. The proposed mechanism for this process, depicted in Scheme 5, involves the stepwise $\kappa^2-\kappa^1$ dissociation of the acetato ligand and coordination of dihydrogen. Heterolytic cleavage of dihydrogen, mediated through either the acetato ligand or NEt_3, and substitution of the chloro ligand by $\kappa^1-\kappa^2$ coordination of acetato ligand then affords **4**. Although the $\kappa^3-\kappa^2$ dissociation of triphos is also conceivable, the proposed mechanism has a literature pre-

(21) Manson, J. *Multinuclear NMR*; Plenum Press: New York, 1987; p 369.

(22) Rhodes, L. F.; Sorato, C.; Venanzi, L. M.; Bachechi, F. *Inorg. Chem.* **1988**, *27*, 604.

(23) (a) Widegren, J. A.; Finke, R. F. *J. Mol. Catal. A: Chem.* **2003**, *198*, 317. (b) Anton, D. R.; Crabtree, R. H. *Organometallics* **1983**, *2*, 855.

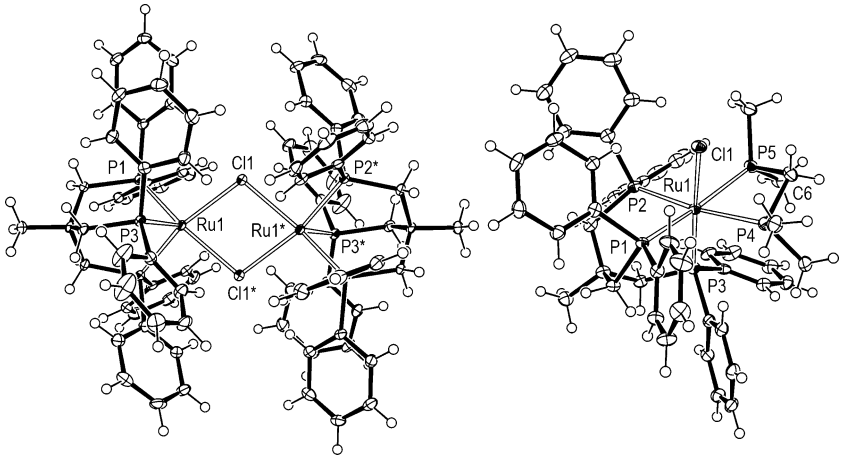

Figure 4. ORTEP representations of **6** and **7** (one of the two molecular units in the asymmetric cell); thermal ellipsoids drawn at 50% probability. Counteranion omitted for clarity. Symmetry equivalent atoms in the structure of **6** labeled with an asterisk (*) were obtained by the symmetry operation $1 - x$, $1 - y$, $1 - z$.

Table 2. Hydrogenation of Alkenes with **1**−**4**[a]

	preparation	alkene	H_2/bar	TOF_{avg}/h^{-1}
1	N_2	styrene	5	6400
2	N_2	styrene	5	3000
2[b]	N_2	styrene	5	2600
3	N_2	styrene	5	8000
4	N_2	styrene	5	<100
1	N_2	styrene	50	10 000
2	N_2	styrene	50	10 000
3	N_2	styrene	50	10 000
1	Air	styrene	50	200
2	Air	styrene	50	7400
3	Air	styrene	50	900
1	N_2	1-hexene	5	9800[c]
2	N_2	1-hexene	5	200[c]
2	N_2	1-hexene	50	6800[c]
3	N_2	1-hexene	5	10 000[c]
1	N_2	cyclohexene	50	200
2	N_2	cyclohexene	50	<100
3	N_2	cyclohexene	50	6200

[a] Conditions: 1.0×10^{-6} mol precatalyst, S:C = 10 000:1, 2 mL of THF, 100 mg of octane (internal standard), 50 °C, 60 min. Conversion determined by GC. Values averaged over duplicate runs. [b] 0.1 mL of Hg added. [c] Isomerization <5% total product (as indicated by the presence of *trans*-2-hexene).

Scheme 4. Reaction of **2** with H_2 in the Presence of NEt_3

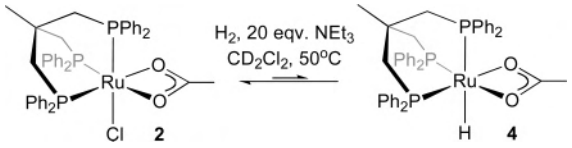

cedent involving reaction of $[Ru(\kappa^1\text{-}O_2CCF_3)(\kappa^2\text{-}O_2CCF_3)(\kappa^3\text{-triphos})]$ with H_2O.[24]

The lack of catalytic activity observed for the hydride analogue **4** suggests that the chloro ligand plays an important, spectator role during catalysis with **2**. Complex **4** is also a valuable model system to gain further insights into the reactivity of **2**. For example, the possibility of dynamic $\kappa^2-\kappa^1$ dissociation of the acetato ligand and dihydrogen coordination in these complexes was investigated by reaction of **4** with deuterium by high-pressure NMR spectroscopy. Under

(24) Herold, S.; Mezzetti, A.; Venanzi, L. M.; Albinati, A.; Lianza, F.; Gerfin, T.; Gramlich, V. *Inorg. Chim. Acta* **1995**, *235*, 215.

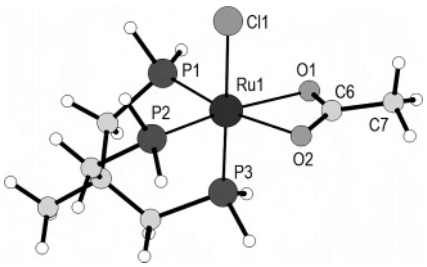

Figure 5. Optimized structure of the model species **I**.

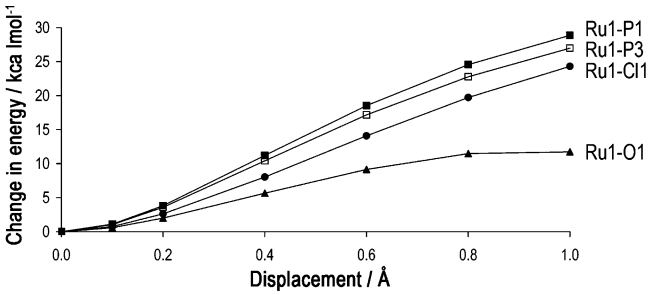

Figure 6. Relaxed potential-energy surfaces for the elongation of metal−ligand bonds in the model species **I**. Labels as defined in Figure 5.

10 bar of D_2 at 50 °C, rapid deuteration ($t_{1/2}$ < 5 min) of the hydride ligand occurs, affording the deuterated complex **9** (Scheme 6). The structure of **9** is further supported by the observation of $^2J_{PD}$ couplings in the $^{31}P\{^1H\}$ NMR spectrum ($^2J_{PD}$(cis) = 3 Hz, $^2J_{PD}$(trans) ≈ 19 Hz). Complex **4** was also found to react with styrene (20 equiv) at room temperature, establishing an equilibrium reaction with the alkyl complex $[Ru(CH_2CH_2Ph)(OAc)(\kappa^3\text{-triphos})]$ (**10**), presumably via κ^2 coordination of the alkene and hydride insertion (**4**:**10** = 4:1, Scheme 6). Complex **10** was identified by the presence of a doublet at 50.7 ppm and triplet at 1.9 ppm in a 2:1 ratio with a $^2J_{PP}$ coupling constant of 20 Hz by $^{31}P\{^1H\}$ NMR spectroscopy (CD_2Cl_2, 293 K). ^1H and ^{13}C NMR spectroscopy also corroborate the structure well, although complete NMR characterization is limited by the presence of an excess of styrene and **4**. The related complex, $[RuH(O_2CCF_3)(PPh_3)_3]$, is known to undergo a similar

Scheme 5. Proposed Mechanism of the Equilibrium between **2** and **4** ([Ru] = [Ru(κ^3-triphos)])

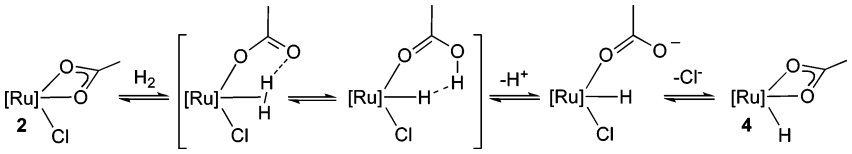

Scheme 6. Reaction of **4** with Deuterium (CD_2Cl_2, 50 °C, 10 bar D_2) and Styrene (CD_2Cl_2, rt, 20 equiv of styrene)

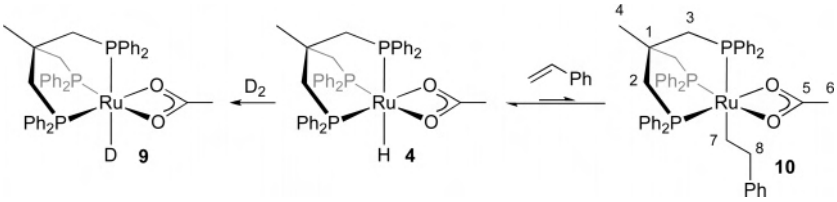

Scheme 7. Proposed Mechanism for the Hydrogenation of Alkenes with **2** (Ru = [RuCl(κ^3-triphos)])

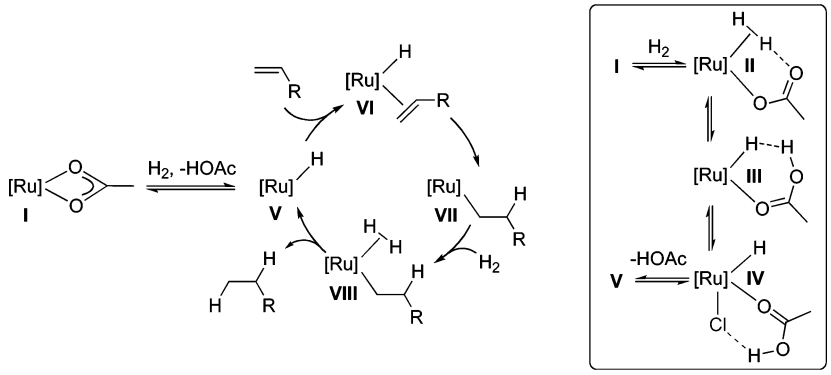

reversible reaction forming [Ru(Et)(O_2CCF_3)(PPh_3)$_3$] upon pressurization with ethylene.[25]

On the basis of the established mechanism for [RuHCl(PPh_3)$_3$][12a,26] and the above experimental observations, the mechanism depicted in Scheme 7 is proposed for hydrogenation of alkenes with **2**. Chloro and triphos ligands are spectator ligands throughout, while the acetato ligand is proposed to play an important role in the formation of the active hydride species **V** by undergoing $\kappa^2-\kappa^1$ dissociation and assisting the heterolytic cleavage of dihydrogen (**II**→**III**).[27] The heterolytic cleavage of dihydrogen with carboxylato ligands has literature precedent in the proposed mechanism of catalysis with [Ru(BINAP)(O_2CR)$_2$].[28] The proposed catalytic cycle comprises a classical inner-sphere, hydride route mechanism involving coordination of the alkene (**VI**), hydride insertion (**VI**→**VII**), coordination of dihydrogen (**VIII**), and σ-bond metathesis (**VIII**→**V**).

The proposed mechanism is supported by a computational analysis using a model system in which the phenyl rings have been replaced by hydrogen atoms ([Ru] = [RuCl(κ^3-(PH_2CH_2)$_3$CMe)] and R = H in Scheme 7). The optimized geometry of the model species **I** (Figure 5) shows good agreement with the structure of **2** determined by X-ray diffraction (Figure 2, comparison of structural parameters in Table 3), verifying the computational procedure (see Experimental Section). One notable difference between these two structures is the lack of significant bending of the chloro ligand out of the axial axis in the calculated structure [P3−Ru1−Cl1 = 178.6 (calcd), 171.06(7)° (expt)]. The absence of this deviation in the model structure, containing a much less sterically demanding triphosphine, strengthens the suggestion that this bending in **2** is the result of steric interactions. Calculated relaxed potential-energy surfaces for elongation of metal−ligand bonds in the model species **I** indicates that the $\kappa^2-\kappa^1$ dissociation of the acetato ligand is the most facile dissociation pathway, in agreement with the proposed mechanism for generation of the active catalytic species (Figure 6).

Calculated Gibbs free energies and geometries of the species involved in the proposed mechanism are depicted in

Table 3. Geometry Comparison between the Model Species **I** and **2**

	bond lengths (Å) and angles (deg)	
	calcd	expt
Ru1−Cl1	2.46	2.448(2)
Ru1−P1	2.27	2.277(3)
Ru1−P2	2.27	2.282(2)
Ru1−P3	2.28	2.275(2)
Ru1−O1	2.19	2.249(5)
Ru1−O2	2.19	2.198(6)
Ru1−C6	2.54	2.580(9)
Ru1−C6−C7	171.4	173.0 (6)
Cl1−Ru1−P3	178.6	171.05 (7)
P1−Ru1−P2	86.7	86.28(8)
P1−Ru1−P3	89.7	89.11(9)
P2−Ru1−P3	90.0	88.37(8)
O1−Ru1−O2	60.2	59.7(2)

(25) Rose, D.; Gilbert, J. D.; Richardson, R. P.; Wilkinson, G. *J. Chem. Soc. A* **1969**, 2610.
(26) Crabtree, R. H. *The Organometallic Chemistry of the Transition Metals*, 4th Ed.; John Wiley & Sons: Hoboken, 2005.
(27) The heterolytic activation of dihydrogen with the acetato ligand is speculative, although it is consistent with the observed reactivity of **2** with acids and the computational analysis.
(28) Ashby, M. T.; Halpern, J. *J. Am. Chem. Soc.* **1991**, *113*, 589.

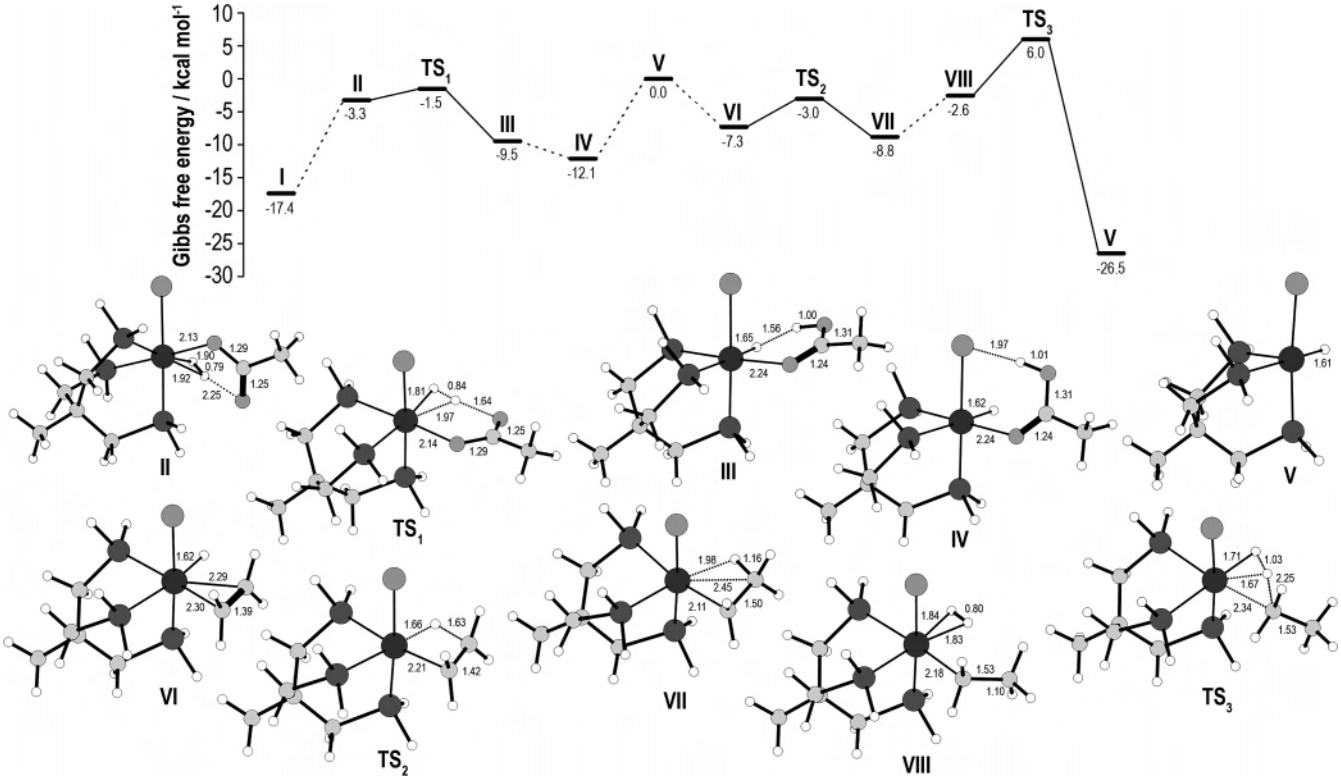

Figure 7. Calculated Gibbs free energies (above) and geometries (below, with key distances in Å) for species involved in the proposed mechanism of alkene hydrogenation with **2**.

Table 4. Crystallographic Data for **2**, **6**, and **7**

	2	**6**	**7**
formula	$C_{43}H_{42}ClO_2P_3Ru$	$C_{82}H_{78}B_2Cl_2F_8P_6Ru_2$	$2C_{46}H_{53}ClF_6P_6Ru{\cdot}3CH_2Cl_2$
MW	820.20	1695.92	2339.23
T [K]	100(2)	100(2)	100(2)
cryst syst	monoclinic	triclinic	triclinic
space group	$P2_1/c$	$P\bar{1}$	$P\bar{1}$
a [Å]	10.082(6)	12.4280(12)	12.473(3)
b [Å]	15.654(8)	12.5183(15)	20.205(4)
c [Å]	27.322(18)	14.0167(18)	22.009(3)
α [deg]		114.580(9)	77.643(11)
β [deg]	96.45(5)	97.356(10)	80.115(15)
δ [deg]		102.402(9)	73.574(14)
V [Å^3]	4285(4)	1877.9(4)	5160.5(16)
Z	4	1	2
density [gcm^{-3}]	1.271	1.500	1.505
μ (mm^{-1})	0.573	0.666	0.752
θ range [deg]	$3.30 \le \theta \le 25.03$	$3.33 \le \theta \le 25.03$	$3.32 \le \theta \le 25.03$
measd reflns	31 611	33 227	10 3188
unique reflns	7426 [$R_{int} = 0.0936$]	6593 [$R_{int} = 0.0806$]	18 099 [$R_{int} = 0.0384$]
no. of data/restr/param	7426/6/453	6593/0/495	18 099/0/1194
$R1$, $wR2$ [$I > 2s(I)$][a]	0.0871, 0.2159	0.0424, 0.0830	0.0435, 0.0938
GoF[b]	1.061	1.088	1.196

[a] $R1 = \sum||F_o| - |F_c||/\sum|F_o|$, $wR2 = \{\sum[w(F_o^2 - F_c^2)^2]/\sum[w(F_o^2)^2]\}^{1/2}$. [b] GoF $= \{\sum[w(F_o^2 - F_c^2)^2]/(n - p)\}^{1/2}$, where n is the number of data and p is the number of parameters refined.

Figure 7. On the basis of these data, the $\kappa^2-\kappa^1$ dissociation of the acetato ligand and coordination of dihydrogen (**I→II**) is suggested to be the limiting step for generation of the active hydride species (**V**), in agreement with the observed pressure dependence on the hydrogenation of 1-alkenes and reactions of dihydrogen with **2**. The heterolytic cleavage of dihydrogen with the κ^1-acetato ligand (**II→III**) is calculated to proceed with a low-energy barrier [1.7 kcal mol^{-1}]. In comparison, the estimated energy barrier for HCl loss is at least 10 times higher on the basis of attempted, although unsuccessful, optimizations of the corresponding transition state. A large energy barrier for complete dissociation of acetic acid is implied from the relative energies of **V** and **IV**,[29] suggesting that acetic acid could compete with coordination of the substrate. Experimentally, this suggestion is supported by the detection of only **2** following hydrogenation of styrene (sample prepared under N_2) and the reversible nature of the reactions of **2** with hydrogen. Competition

(29) This aspect is probably overestimated in the gas phase.

should be more pronounced for larger substrates, owing to the steric bulk of the triphos ligand, and thus, acetic acid coordination could be the reason for the low activity observed for cyclohexene with **2**. The rate-determining step for the catalytic cycle is suggested to be the σ-bond metathesis, consistent with that suggested for $[RuHCl(PPh_3)_3]$,[12a] as this step has the highest calculated energy barrier in the cycle.

Concluding Remarks

Aspects of the reactivity and catalytic activity of the ruthenium(II)−triphos acetato complex $[RuCl(OAc)(\kappa^3\text{-triphos})]$ have been established. Substitution of the acetato ligand in $[RuCl(OAc)(\kappa^3\text{-triphos})]$ is readily effected by treatment with acid, affording $[Ru_2(\mu\text{-Cl})_3(\kappa^3\text{-triphos})_2]Cl$ and the 16 VE dimer $[RuCl(\kappa^3\text{-triphos})]_2(BF_4)_2$ with aqueous HCl and $[Et_2OH]BF_4$, respectively. Substitution of the acetato ligand can also be effected by heating with a basic diphosphine, dmpm, in the presence of $[NH_4]PF_6$, resulting in formation of $[RuCl(\kappa^2\text{-dmpm})(\kappa^3\text{-triphos})]PF_6$. Although no new products are apparent on pressurization of $[RuCl(OAc)(\kappa^3\text{-triphos})]$ with dihydrogen and heating to 50 °C, supplementary experiments with added base and deuteration experiments of the related hydride complex $[RuH(OAc)(\kappa^3\text{-triphos})]$ indicate the presence of reversible and rapid processes involving $\kappa^2-\kappa^1$ dissociation of the acetato ligand and coordination of dihydrogen.

Catalytic experiments with $[RuCl(OAc)(\kappa^3\text{-triphos})]$ demonstrated the high activity of this complex for hydrogenation of 1-alkenes. While less active than the related compounds $[RuCl(OAc)(PPh_3)_3]$ and $[RuCl_2(PPh_3)_3]$, the triphos complex showed much greater tolerance to air. For experiments carried out at 50 °C with 50 bar of H_2 in THF (samples prepared under N_2), TOFs of ≥10 000 (7400 h^{-1} for samples prepared in air) and 6800 h^{-1} could be obtained for hydrogenation of styrene and 1-hexene, respectively. The hydride complex, $[RuHCl(\kappa^3\text{-triphos})]$, formed by acetato-mediated heterolytic cleavage of dihydrogen is proposed as the active catalytic species. An inner-sphere, hydride route mechanism is suggested for the catalytic cycle, with chloro and triphos ligands playing a spectator role. These mechanistic proposals are consistent with reactivity studies carried out on $[RuCl(OAc)(\kappa^3\text{-triphos})]$ and $[RuH(OAc)(\kappa^3\text{-triphos})]$ and supported by a computational analysis.

Experimental Section

All organometallic manipulations were carried out under a nitrogen atmosphere using standard Schlenk techniques. CH_2Cl_2, toluene, diethyl ether, and THF were dried under nitrogen using a solvent purification system, manufactured by Innovative Technology Inc. Octane was distilled from CaH_2 and stored over molecular sieves under nitrogen. CD_2Cl_2 (for NMR experiments under N_2) was distilled from CaH_2 and stored under nitrogen. All other solvents were p.a. quality and saturated with nitrogen prior to use. Styrene, 1-hexene, and cyclohexene were saturated with nitrogen and stored over molecular sieves. $[RuCl(OAc)(PPh_3)_3]$[17] and $[RuH(OAc)(PPh_3)_3]$[30] were prepared as described elsewhere. All other chemicals are commercial products and used as received (including $[RuCl_2(PPh_3)_3]$, Fluka). NMR spectra were recorded on a Bruker Avance 400 MHz spectrometer at room temperature unless otherwise stated. Chemical shifts are given in ppm and coupling constants (J) in Hz. High-pressure in situ NMR measurements were performed in sapphire NMR tubes.[31] Simulation analysis of the $^{31}P\{^1H\}$ NMR spectrum of **7** was carried out using *g*-NMR.[32] The NMR labeling schemes for **2** and **4** (Scheme 2), **6** and **7** (Scheme 3), and **10** (Scheme 6) have been previously detailed. ESI-MS were recorded on a Thermo Finnigan LCQ DecaXP Plus quadrupole ion trap instrument using a literature protocol.[33] Microanalyses were performed at the EPFL.

Preparation of $[RuCl(OAc)(\kappa^3\text{-triphos})]$ (2). A suspension of $[RuCl(OAc)(PPh_3)_3]$ (2.50 g, 2.54 mmol) and $(PPh_2CH_2)_3CMe$ (1.59 g, 2.54 mmol) in toluene (100 mL) was heated under reflux for 30 min. The solution was then cooled to RT, and the product, as a yellow powder, was isolated by filtration and washed with toluene (3 × 50 mL) and diethyl ether (3 × 50 mL). Yield: 1.94 g (93%). Yellow crystals suitable for X-ray diffraction were obtained from a CH_2Cl_2 solution layered with cyclohexane at RT. ^1H NMR (CD_2Cl_2, 400 MHz, 263 K): δ 6.80−7.84 (m, 30H), 2.18−2.36 (m, 6H, $H^2 + H^3$), 1.97 (s, 3H, H^6), 1.53 (br, 3H, H^4). $^{13}C\{^1H\}$ NMR (CD_2Cl_2, 100 MHz, 263 K): δ 186.5 (br, C^5), 127−138 (m), 37.8 (q, $^2J_{PC} = 3$, C^1), 37.5 (q, $^3J_{PC} = 10$, C^4), 33.0 (br d, $^1J_{PC} = 32$, C^3), 32.1 (br t, $^3J_{PC} = 20$, C^2), 25.7 (s, C^6). $^{31}P\{^1H\}$ NMR (CD_2Cl_2, 162 MHz, 263 K): δ 40.4 (d, $^2J_{PP} = 40$, 2P, Ru−PPh$_2$C^2), 37.0 (t, $^2J_{PP} = 40$, 1P, Ru−PPh$_2$C^3). Anal. Calcd for $C_{43}H_{42}ClO_2P_3Ru$ (820.25 g mol^{-1}): C, 62.97; H, 5.16. Found: C, 62.98; H, 5.26.

Preparation of $[RuH(OAc)(\kappa^3\text{-triphos})]$ (4). A suspension of $[RuH(OAc)(PPh_3)_3]$ (0.30 g, 0.38 mmol) and $(PPh_2CH_2)_3CMe$ (0.24 g, 0.38 mmol) in toluene (30 mL) was heated under reflux for 30 min. The solution was then cooled to RT, and the product was isolated, as yellow powder, by filtration and washed with toluene (2 × 10 mL) and diethyl ether (2 × 10 mL). Yield: 0.15 g (50%). ^1H NMR (CD_2Cl_2, 400 MHz): δ 6.87−7.82 (m, 30H), 2.23−2.34 (m, 2H, H^3), 2.23 (br d, $^2J_{HH} = 16$, 2H, H^2), 2.14 (br d, $^2J_{HH} = 16$, 2H, $H^{2'}$), 2.03 (s, 3H, H^6), 1.53 (s, 3H, H^4), −2.78 (dt, $^2J_{PH} = 122$, $^2J_{PH} = 20$, 1H, Ru−H). $^{13}C\{^1H\}$ NMR (CD_2Cl_2, 100 MHz): δ 182 (C^5), 126−140 (m), 39 (br, C^1), 37.9 (q, $^3J_{PC} = 10$, C^4), 35.3 (dt, $^1J_{PC} = 22$, $^3J_{PC} = 3$, C^3), 33.5 (td, $^3J_{PC} = 18$, $^1J_{PC} = 5$, C^2), 24.1 (s, C^6). $^{31}P\{^1H\}$ NMR (CD_2Cl_2, 162 MHz): δ 61.0 (d, $^2J_{PP} = 20$, 2P, Ru−PPh$_2$C^2), 6.4 (t, $^2J_{PP} = 20$, 1P, Ru−PPh$_2$C^3). Anal. Calcd for $C_{43}H_{43}O_2P_3Ru$ (785.80 g mol^{-1}): C, 65.73; H, 5.52. Found: C, 65.45; H, 5.54.

Preparation of $[Ru_2(\mu\text{-Cl})_3(\kappa^3\text{-triphos})]Cl$ (5) from $[RuCl(OAc)(\kappa^3\text{-triphos})]$ (2). A biphasic mixture of $[RuCl(OAc)(\kappa^3\text{-triphos})]$ (0.10 g, 0.12 mmol) in CH_2Cl_2 (20 mL) and aqueous HCl (100 mM, 20 mL) was stirred vigorously at RT for 1 h. The organic phase was separated, washed with H_2O (3 × 50 mL), and then dried with Na_2SO_4. The product was obtained as a microcrystalline yellow solid by recrystallization from CH_2Cl_2−hexane. Yield: 0.078 g (81%). NMR data are in agreement with the literature data.[34]

Preparation of $[RuCl(\kappa^3\text{-triphos})]_2(BF_4)_2$ (6). To a solution of $[RuCl(OAc)(\kappa^3\text{-triphos})]$ (0.20 g, 0.24 mmol) in CH_2Cl_2 (20 mL), cooled to −78 °C, $HBF_4{\cdot}OEt_2$ (0.035 mL, 0.26 mmol) was added, and the solution was stirred for 5 min before slowly warming to RT and stirring for a further 30 min. The product was then

(30) Mitchell, R. W.; Spencer, A.; Wilkinson, G. *J. Chem. Soc., Dalton Trans.* **1973**, 846.
(31) Cusanelli, A.; Frey, U.; Richens, D. T.; Merbach, A. E. *J. Am. Chem. Soc.* **1996**, *118*, 5265.
(32) Budzelaar, P. H. M. *g-NMR*, v4.0; IvorySoft, 1997.
(33) Dyson, P. J.; McIndoe, J. S. *Inorg. Chim. Acta* **2003**, *354*, 69.
(34) Rhodes, L. F.; Sorato, C.; Venanzi, L. M.; Bachechi, F. *Inorg. Chem.* **1988**, *27*, 604.

precipitated by addition of toluene (20 mL). The microcrystalline orange solid was then washed with toluene (2 × 10 mL) and diethyl ether (10 mL) and dried in vacuo. Yield: 0.14 g (68%). Red crystals suitable for X-ray diffraction were obtained from a CH_2Cl_2 solution layered with diethyl ether at RT. ^{1}H NMR (CD_2Cl_2, 400 MHz, N_2): δ 6.90−7.37 (m, 30H), 2.62−2.70 (m, 6H, H^2), 1.86−1.92 (m, 3H, H^3). ^{13}C{^{1}H} NMR (CD_2Cl_2, 100 MHz, N_2): δ 128−133 (m), 41.4 (br, C^1), 36.0−36.4 (m, C^3), 33.9−34.5 (m, C^2). ^{31}P{^{1}H} NMR (CD_2Cl_2, 162 MHz, N_2): δ 55.8 (s, 6P). ^{11}B{^{1}H} NMR (CD_2Cl_2, 128 MHz, N_2): δ −1.1 (s, BF_4). ESI-MS (CH_2Cl_2, 60 °C, 5.0 kV) positive ion, *m*/*z*, 761 $[M]^{2+}$; negative ion, *m*/*z*, 87 $[BF_4]^-$. Anal. Calcd for $C_{82}H_{78}B_2Cl_2F_8P_6Ru_2$ (1696.02 g mol^{-1})·$^1/_2$(CH_2Cl_2): C, 56.48; H, 4.55. Found: C, 56.50; H, 4.71

Preparation of [RuCl(κ^2-dmpm)(κ^3-triphos)]PF_6 (7). To a suspension of [RuCl(OAc)(κ^3-triphos)] (0.10 g, 0.12 mmol) and $[NH_4]PF_6$ (0.03 g, 0.18 mmol) in CH_2ClCH_2Cl (10 mL), $Me_2PCH_2PMe_2$ (0.022 mL, 0.14 mmol) was added. The suspension was heated at 50 °C for 3 h and then filtered. The filtrate was concentrated to ca. 1 mL, and the product was precipitated by addition of excess diethyl ether (50 mL). The precipitate was then washed with diethyl ether (3 × 20 mL) and dried in vacuo. Yield: 0.11 g (90%) as a pale yellow powder. Yellow crystals suitable for X-ray diffraction were obtained from a CH_2Cl_2 solution layered with hexane at RT. ^{1}H NMR (CD_2Cl_2, 400 MHz): δ 6.73−7.77 (m, 30H), 4.11−4.30 (m, 1H, H^5), 2.70−2.86 (m, 1H, $H^{5'}$), 2.48 (br d, $^2J_{PH}$ = 8, 2H, H^3), 2.40−2.50 (m, 2H, H^2), 2.25−2.40 (m, 2H, $H^{2'}$), 1.77−1.86 (m, 6H, P*Me*$_2$), 1.46 (br, 3H, H^4), 0.85−0.94 (m, 6H, P*Me*$'_2$). ^{13}C{^{1}H} NMR (CD_2Cl_2, 100 MHz): δ 127−140 (m), 45.4 (t, $^1J_{PC}$ = 29, C^5), 41.1 (dt, $^1J_{PC}$ = 27, $^3J_{PC}$ = 6, C^3), 38.0 (q, $^3J_{PC}$ = 10, C^4), 36.4−36.5 (m, C^1), 31.3−31.8 (m, C^2), 16.5−17.0 (m, P*Me*$'_2$), 14.5−14.9 (m, P*Me*$_2$). ^{31}P{^{1}H} NMR (CD_2Cl_2, 162 MHz): δ 40.9−41.9 (m, 1P, Ru−*P*Ph_2C^3), 1.6−4.8 (m, 2P, Ru−*P*Ph_2C^2), −39.2 to −36.1 (m, 2P, Ru−*P*Me_2), −145.2 (sept, $^1J_{PF}$ = 711, 1P, *P*F_6). ESI-MS (CH_2Cl_2, 60 °C, 5.0 kV) positive ion, *m*/*z*, 897 $[M]^+$; negative ion, *m*/*z*, 145 $[PF_6]^-$. Anal. Calcd for $C_{46}H_{53}ClF_6P_6Ru$ (1042.28 g mol^{-1}): C, 53.01; H, 5.13. Found: C, 52.75; H, 5.13.

Reactions of [RuCl(OAc)(κ^3-triphos)] (2) with H_2. Reactions of **2** were carried out in sapphire NMR tubes and analyzed by NMR spectroscopy. All manipulations were carried out under a nitrogen atmosphere.

(a) Attempted reaction with H_2: 0.45 mL of a CD_2Cl_2 (0.7 mL) solution of **2** (10 mg) was pressurized under H_2 (50 bar) and heated at 50 °C for 30 min. No reaction was observed.

(b) Reaction with H_2 and NEt_3: 0.45 mL of a CD_2Cl_2 (0.7 mL) solution of **2** (12.5 mg) and NEt_3 (0.04 mL, 20 equiv) was pressurized under H_2 (50 bar) and heated at 50 °C for 30 min, resulting in formation of a small quantity of **4** (**2**:**4** = 12:1). The solution was cooled to RT and pressurized with further H_2 (to 80 bar) and heated again at 50 °C for 30 min (**2**:**4** = 10:1). The solution was cooled to RT and after releasing the pressure degassed by bubbling with N_2, which resulted in the removal of peaks attributed to **4** in the NMR spectra.

Reactions of [RuH(OAc)(κ^3-triphos)] (4). All manipulations were carried out under a nitrogen atmosphere.

(a) Reaction with NEt_3·HCl: To a solution of **4** (3 mg) in CD_2Cl_2 (0.5 mL), NEt_3·HCl (∼3 equiv) was added. ^{31}P{^{1}H} and ^{1}H NMR spectroscopy indicated that **2** was formed quantitatively. A trace quantity of H_2 was detected by the presence of weak singlet at 4.64 ppm by ^{1}H NMR spectroscopy.

(b) Reaction with D_2: 0.45 mL of a CD_2Cl_2 (0.7 mL) solution of **4** (8 mg) was added to a sapphire NMR which was sealed and pressurized with D_2 (10 bar) then heated at 50 °C. Rapid deuteration of the hydride resonance is observed ($t_{1/2}$ < 5 min). ^{31}P{^{1}H} NMR (CD_2Cl_2, 162 MHz, D_2): δ 61.1 (dt, $^2J_{PP}$ = 20, $^2J_{PD}$ = 3, 2P, Ru−*P*Ph_2C^2), 6.2 (virtual pentet, J = 19, 1P, Ru−*P*Ph_2C^3)

(c) Reaction with $PhCHCH_2$: A solution of **4** (8 mg) and $PhCHCH_2$ (0.02 mL, 20 equiv) in CD_2Cl_2 (0.7 mL) was analyzed by NMR spectroscopy. Formation of a small amount of new species was observed and assigned to [Ru(CH_2CH_2Ph)(OAc)(κ^3-triphos)] (**10**) by NMR spectroscopy (see below).[35] The ratio of **4**:**10** was constant at 4:1, despite the large excess of $PhCHCH_2$, by both ^{1}H and ^{31}P{^{1}H} NMR spectroscopy. ^{1}H NMR (CD_2Cl_2, 400 MHz, N_2): δ 6.87−7.82 (m, obscured, *Ph*), 2.66−2.76 (m, 2H, H^8), 2.44−2.54 (m, 2H, H^2), 2.3−2.37 (m, obscured, $H^{2'}$ + H^3), 2.15 (s, 3H, H^6), 1.62 (br, 3H, H^4), 1.44−1.52 (m, 2H, H^7). ^{13}C{^{1}H} NMR (CD_2Cl_2, 100 MHz, N_2, selected peaks only): δ 183 (C^5), 39 (C^4), 38 (C^8), 35 (C^7, tentative), 35 (C^2), 25 (C^6). ^{31}P{^{1}H} NMR (CD_2Cl_2, 162 MHz, N_2): δ 50.7 (d, $^2J_{PP}$ = 20, 2P, Ru−*P*Ph_2C^2), 1.9 (t, $^2J_{PP}$ = 20, 1P, Ru−*P*Ph_2C^3).

Catalytic Evaluations. All catalytic experiments were conducted using a home-built multicell autoclave containing an internal temperature probe. Each glass reaction vessel was charged with the precatalyst, substrate, internal standard (100 mg octane), and solvent and then placed inside the autoclave and sealed. This procedure was either carried out in air or a glove box (general procedure). Following flushing with H_2 (desired pressure 5 bar, 4 × 5 bar; otherwise, 3 × 10 bar), the autoclave was heated to 50 °C under H_2 (desired pressure 5 bar, 5 bar; desired pressure 50 bar, 10 bar) and then maintained at the desired pressure for the duration of the catalytic run. The autoclave was then cooled to ambient temperature (typically ≤5 min) using an external water-cooling jacket and the pressure released. Conversions were determined by GC analysis of the samples using a Varian chrompack CP-3380 gas chromatograph with species verified by comparison to authentic samples.

Computational Methods. All geometry optimizations and frequency calculations were carried out using the Gaussian03 suite of programs.[36] Density functional theory using the hybrid B3LYP functional and pruned grid consisting of 75 radial shells and 302 angular points was used for all geometry optimizations and frequency calculations. The 6-31G(d,p) basis set used for all atoms except Ru, for which the LanL2DZ basis set and pseudo potentials were used. The nature of each of the stationary points was determined by vibrational analysis. Energies for the small molecules used in this study and the optimized geometries and energies of model complexes (together with relaxed potential energy surface data) are collected in Tables S1−S3.

(35) Assignment notes: (a) a $^3J_{HH}$ coupling was detected between H^7 and H^8 by COSY; (b) a $^3J_{PC}$ coupling was detected between H^8 and a Ph peak at 128 ppm by C,H long-range correlation spectroscopy.

(36) Frisch, M. J.; Trucks, G. W.; Schlegel, H. B.; Scuseria, G. E.; Robb, M. A.; Cheeseman, J. R.; Montgomery, J. A., Jr.; Vreven, T.; Kudin, K. N.; Burant, J. C.; Millam, J. M.; Iyengar, S. S.; Tomasi, J.; Barone, V.; Mennucci, B.; Cossi, M.; Scalmani, G.; Rega, N.; Petersson, G. A.; Nakatsuji, H.; Hada, M.; Ehara, M.; Toyota, K.; Fukuda, R.; Hasegawa, J.; Ishida, M.; Nakajima, T.; Honda, Y.; Kitao, O.; Nakai, H.; Klene, M.; Li, X.; Knox, J. E.; Hratchian, H. P.; Cross, J. B.; Bakken, V.; Adamo, C.; Jaramillo, J.; Gomperts, R.; Stratmann, R. E.; Yazyev, O.; Austin, A. J.; Cammi, R.; Pomelli, C.; Ochterski, J. W.; Ayala, P. Y.; Morokuma, K.; Voth, G. A.; Salvador, P.; Dannenberg, J. J.; Zakrzewski, V. G.; Dapprich, S.; Daniels, A. D.; Strain, M. C.; Farkas, O.; Malick, D. K.; Rabuck, A. D.; Raghavachari, K.; Foresman, J. B.; Ortiz, J. V.; Cui, Q.; Baboul, A. G.; Clifford, S.; Cioslowski, J.; Stefanov, B. B.; Liu, G.; Liashenko, A.; Piskorz, P.; Komaromi, I.; Martin, R. L.; Fox, D. J.; Keith, T.; Al-Laham, M. A.; Peng, C. Y.; Nanayakkara, A.; Challacombe, M.; Gill, P. M. W.; Johnson, B.; Chen, W.; Wong, M. W.; Gonzalez, C.; Pople, J. A. *Gaussian 03*, Revision D.01; Gaussian, Inc.: Wallingford, CT, 2004.

Crystallography. Relevant details about the structure refinements are given in Table 4. Data collection for the X-ray structure determinations was performed on a BRUKER APEX II CCD diffractometer system using graphite-monochromated Mo Kα radiation (0.71073 Å) and a low-temperature device. Data reduction was performed using EvalCCD.[37] Structures were solved using SIR97[38] and refined (full-matrix least-squares on F^2) using SHELX-TL.[39] An absorption correction (multiscan, SADABS) was applied to the data sets of **6** and **7**.[40] All non-hydrogen atoms were refined anisotropically with hydrogen atoms placed in calculated positions using the riding model. Problematic solvent disorder in the solution of **2** was treated using the SQUEEZE algorithm.[41] The $[BF_4]^-$ counterion in **6** was split over two sites as was one solvent molecule in **7**. Restrains were made to the displacement parameters of some of the atoms of these disordered molecules and one atom in a phenyl ring of **2**. Graphical representations of the structures were made with ORTEP3.[42]

Acknowledgment. This work was supported by the EPFL and the Swiss National Science Foundation. We are grateful to Dr. Rosario Scopelliti and Dr. E. Solari for assistance with crystallography. We also thank the New Zealand Foundation for Research, Science and Technology for a Top Achiever Doctoral Fellowship (A.B.C.).

Supporting Information Available: Crystallographic information for **2**, **6**, and **7** (CIF format) and Tables S1−S3. This material is available free of charge via the Internet at http://pubs.acs.org.

IC701773A

(37) Duisenberg, A. J. M.; Kroon-Batenburg, L. M. J.; Schreurs, A. M. M. *J. Appl. Crystallogr*. **2003**, *36*, 220; Bruker AXS, Inc.: Madison, WI, 1997.
(38) Altomare, A.; Burla, M. C.; Camalli, M.; Cascarano, G. L.; Giacovazzo, C.; Guagliardi, A.; Moliterni, A. G. G.; Polidori, G.; Spagna, R. *J. Appl. Crystallogr*. **1999**, *32*, 115.
(39) Sheldrick, G. M. *SHELXTL*; University of Göttingen: Göttingen, Germany, 1997; Bruker AXS, Inc.: Madison, WI, 1997.
(40) Bruker AXS, Inc.: Madison, WI, 1997.
(41) (a) Spek, A. L. *PLATON, A Multipurpose Crystallographic Tool*; Utrecht University: The Netherlands, 2007. (b) Spek, A. L. *J. Appl. Crystallogr*. **2003**, *36*, 7.
(42) Farrugia, L. J. *J. Appl. Crystallogr*. **1997**, *30*, 565.